DOI: 10.1007/s12541-015-0162-6 ISSN 2234-7593 (Print) / ISSN 2005-4602 (Online)

Thermobattery based on CNT Coated Carbon Textile and Thermoelectric Electrolyte

Kyoung Min Bae[1], Hee Doo Yang[2], Lemma Teshome Tufa[1], and Tae June Kang[1,2,#]

1 Department of Nanofusion Technology, Pusan National University, 2, Busandaehak-ro 63beon-gil, Geumjeong-gu, Busan, 609-735, South Korea
2 Department of Nanomechatronics Engineering, Pusan National University, 2, Busandaehak-ro 63beon-gil, Geumjeong-gu, Busan, 609-735, South Korea
Corresponding Author / E-mail: tjkang@pusan.ac.kr, TEL: +82-51-510-7411, FAX: +82-51-510-7411

KEYWORDS: Thermoelectric effect, Potassium ferri/ferrocyanide, Carbon nanotube, Carbon textile

In this work, we report a thermobattery that can efficiently harvest low-grade waste heat. The thermobattery utilizes temperature dependence of ferri/ferrocyanide ($Fe(CN)_6^{3-}$/$Fe(CN)_6^{4-}$) redox potential and employs the porous carbon textile electrode that is coated with single-walled carbon nanotube (SWNT). Simple and scalable dipping and drying process was applied to prepare the SWNT coated textile electrodes (SWNT-CT). The SWNT coating not only decreases the sheet conductance of the textile remarkably but also provides the number of available reaction sites for thermogalvanic conversion, resulting in improving electrical outputs. The capability for power generation in the thermobattery was quantitatively investigated by measuring potential versus current curves. Discharge behavior of the thermobattery was also discussed to provide an understanding of the internal resistances that limit output electrical power.

Manuscript received: October 24, 2014 / Revised: February 26, 2015 / Accepted: March 1, 2015

1. Introduction

Waste heat is mainly produced by power plants, industrial processes as well as home appliances and usually released to the surrounding environment.[1-5] Sources of waste heat also include all manner of human activities, natural systems, and all organisms.[1-5] As part of an effort to improve energy efficiency, numerous advances have been made in small-scale thermal energy harvesting.[3-12] Among these technologies, thermoelectric generators based on thermoelectrics, metal/semiconductor thermocouples and ferromagnetic materials, etc, have been envisioned as a host for harvesting such low-grade thermal energy.[6,13-15] However, low thermopower (typically several tens and hundreds of microvolts per Kelvin),[6,16] mechanical fragility and high unit cost of electric power have hindered their diverse applicability in harvesting of waste heat.

Despite its relatively low energy efficiency in thermoelectric conversions, liquid thermoelectric devices (i.e., thermal electrochemical cells or thermocells) have recently attracted large amount of attention in scavenging low-grade waste thermal energy with great advantages of high thermopower, simple design, low expected maintenance and low cost.[16-19] The thermoelectric coefficient in liquid thermoelectrics is several times higher than of solid thermoelectrics. Moreover, researchers have become interested in not only focusing on increasing energy conversion efficiency but also on finding cheaper and efficient electrolyte and electrode materials to make these systems cost competitive with conventional solid thermoelectric devices.[16, 20-23]

The present thermobattery utilizes temperature dependence of ferri/ferrocyanide ($Fe(CN)_6^{3-}$/$Fe(CN)_6^{4-}$) redox potential and employs the high specific surface area of carbon textile electrode that is coated with single-walled carbon nanotube (SWNT). Simple and scalable dipping and drying process was applied to prepare the SWNT coated textile electrodes using a highly dispersed SWNT colloidal solution. An electrical output power from the thermobattery was quantitatively investigated by measuring voltage and current curves. Discharge behavior of the thermobattery was also discussed to provide an understanding of the internal resistances that limit output electrical power.

2. Experimental

2.1 Preparation of SWNT coated carbon textile electrodes

SWNT coatings on carbon textile were performed via a dipping and drying process, similar to those widely used for dyeing fibers and fabrics in the textile industry.[24,25] A well-dispersed SWNT colloidal

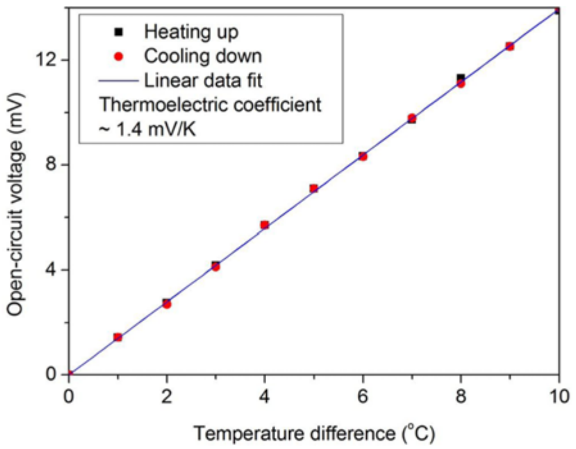

Fig. 1 Thermoelectric coefficient of the redox couple, obtained by measuring the temperature dependence of the potential difference over a temperature range from 0 to 10°C

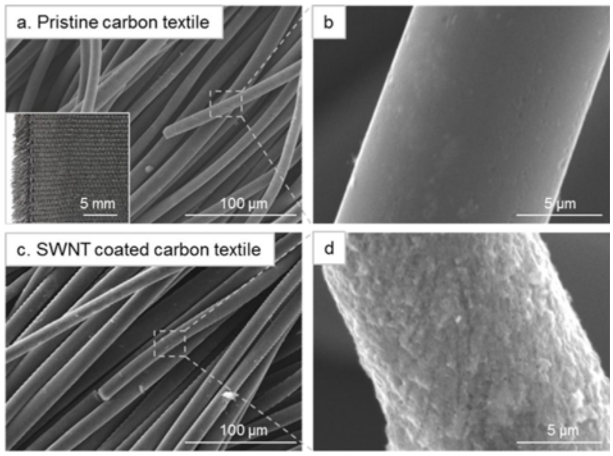

Fig. 2 SEM images of carbon textile before and after SWNT coating. The inset of Fig. 1(a) shows optical image of carbon textile

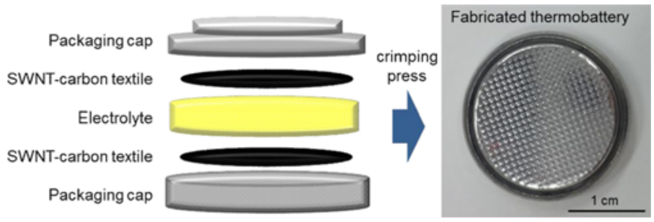

Fig. 3 Schematic assembly and optical image of the thermobattery

solution is prerequisite to achieve uniform coating of SWNTs on carbon textile. In order to prepare stable dispersions of SWNTs, the repulsion forces should overcome the van der Waals forces between the SWNTs and their zeta potentials.[26,27] Therefore, SDBS (sodium dodecylbenzene sulfonate) as an anionic surfactant was used to functionalize the SWNT sidewalls non-covalently.[28,29] The treatment leads to a stable dispersion of SWNTs in aqueous solution by electrostatic repulsions.

SDBS surfactant was dissolved in DI (deionized) at a concentration of 57.4 mM and then purified SWNT powder (ASP-100F, Hanwha Nanotech) was added in the solution. The mixture solution was sonicated for 5 hours, resulting in a highly dispersed SWNT colloidal solution. After preparing the SWNT colloidal solution with a concentration of 2.0 mg/mL, the carbon textile was simply dipped into the solution for SWNT coatings. Due to highly porous structure of carbon textile as shown in Fig. 1(a) and the inset of the Fig., the textile quickly swelled with large amounts of the SWNT solution, which leads to the ease-of-adaptation of a dipping and drying process. The carbon textile was subsequently dried for 1 hour in a chamber at 80°C to evaporate the water. Finally, the SDBS residue remained on the sidewalls of SWNT was washed out using DI water more than three times. Fig. 1 shows scanning electron microscopy (SEM) images of carbon textile before and after SWNT coating. While smooth surface was observed on pristine carbon fiber (see Fig. 1(a) and (b)), SWNT networks was formed conformally on the surface of individual carbon fibers (Fig. 1(c) and (d)). The observed uniform and conformal coating morphology may arise from the large van der Waals interactions between SWNTs and carbon textiles as well as the mechanical flexibility of SWNTs, allowing them to conformally adhere to the surface.

2.2 Preparation of thermoelectric electrolyte and measurement of thermoelectric coefficient

0.4 M potassium ferri/ferrocyanide (Sigma Aldrich) aqueous solution, with concentration close to saturation, was used for the thermoelectric electrolyte. The electrolyte was prepared using DI water and degassed before use by bath sonication. The freshly prepared electrolytes were immediately incorporated into thermobattery before the commencement of a series of measurements to avoid the effect of electrolyte degradation.

Thermoelectric coefficient of the redox couple was obtained by measuring the temperature dependence of the potential difference over a temperature range from 0 to 10°C. As shown in Fig. 2, a linear dependency of the generated open-circuit voltage with respect to the temperature difference was clearly observed without any hysteresis during heating up and cooling down cycles. The slope of the curve (i.e., thermoelectric coefficient) was calculated as being ~1.4 mV/K, which is in good agreement with previous reports.[17,19] It is noteworthy that the thermopower of 1.4 mV/K reaches over 4 times higher than that of bismuth telluride (~300 μV/K) which has been a widely used material for thermoelectric energy conversion.[6,16]

2.3 Fabrication of thermobattery

The present thermobattery has a simple structure consisting of ferri/ferrocyanide redox couple used as thermoelectric electrolyte and SWNT coated carbon textiles (SWNT-CT) as electrodes. Fig. 3 shows the schematic assembly and optical image of the thermobattery. Coin-type cells were constructed using the SWNT-CT electrodes in 2032 (20 mm diameter and 3.2 mm thick) coin cell hardware. The electrodes were attached to package caps with carbon paste, and then the electrolyte was contained in the bottom packaging substrates. Finally, the coin cell was completely sealed by crimping (hydraulic crimping machine, MTI Corporation).

3. Results and Discussion

The present thermobattery is basically relevant to a thermal electrochemical cell utilizing temperature dependence of the redox potential of electrolyte. Upon applying the temperature difference between the inter-electrodes, the thermobattery generates an electrical potential difference that is linearly proportional to the temperature difference as shown in Fig. 2. When the battery is connected to an external electrical load, the thermally generated potential drives electrons in the external circuit and ions in the electrolyte so that electrical current and power can be delivered. Continuous operation of the battery requires diffusion of the reaction product formed at one electrode to the other electrode, where it can then become a reactant.[19] Convective transport of electrolyte ions (i.e., ferri/ferrocyanide ions) can be a useful mode of transport, which is spontaneously generated due to the density gradient of electrolyte between hot and cold electrodes in the thermobattery.[19]

The capability for power generation depends not only on the potential but also on the current delivery characteristics of the thermobattery. The electrode performance to improve discharge behavior is dominantly related to specific surface area of electrode. As shown in the optical and SEM images of Fig. 1(a), carbon textiles have a hierarchically porous structure with micro-scale fibers woven into a textile. The textile structure is able to provide not only a high specific surface area for electrochemical reactions, but also allow efficient mass transport of redox ions. Power generation of the thermobattery with carbon textile and flat stainless steel (SS) electrodes was compared to provide the effectiveness of carbon textile electrode, as shown in Fig. 4. Both electrodes of carbon textile and stainless steel have an identical electrode area of 3.14 cm^2 and the electrode spacing was set to ~3 mm limited by the thickness of the coin cell hardware. The open-circuit voltage from thermobattery was maintained at 10 mV, corresponding to applied temperature difference between two electrodes of ~7.14°C.

The discharge behavior could be evaluated from experimental characteristic curves of potential difference, E, versus current, I curve, as shown in Fig. 4(a). Measured currents were normalized with the electrode size. As shown clearly in the figure, the short-circuit current and discharge behavior is significantly affected by the electrode. When the carbon textile electrode was employed, the short-circuit current increased 2 times as compared with that of stainless steel from 0.14 to 0.3 mA/cm^2. Fig. 4(b) shows the specific output power obtained from the E-I curve. As expected, 2 times higher output power could be delivered as the carbon textile electrode was used.

From the preliminary electrode test in Fig. 4, it is clearly seen that an increase of electrode size can directly increase the number of available reaction sites, so that the thermobattery generates a higher electrical output. To further improve the electrode performance, SWNT coatings on carbon textile were carried out. SWNTs have been widely employed in electrochemical applications due to fast carrier transportation, superior chemical stability, and excellent catalytic activity.[30,31] Therefore, the performance of the device would be enhanced by incorporating SWNT into carbon textile. Fig. 5(a) shows the variation of sheet resistance of carbon textile with respect to the SWNT coating number. As shown in the figure, the sheet resistance of the carbon textile decreased remarkably as the SWNT coating number increased, showing ~1.5 reduction in sheet resistances from 25.8 to 17.6 ohm/sq. upon performing 4 times of SWNT coatings.

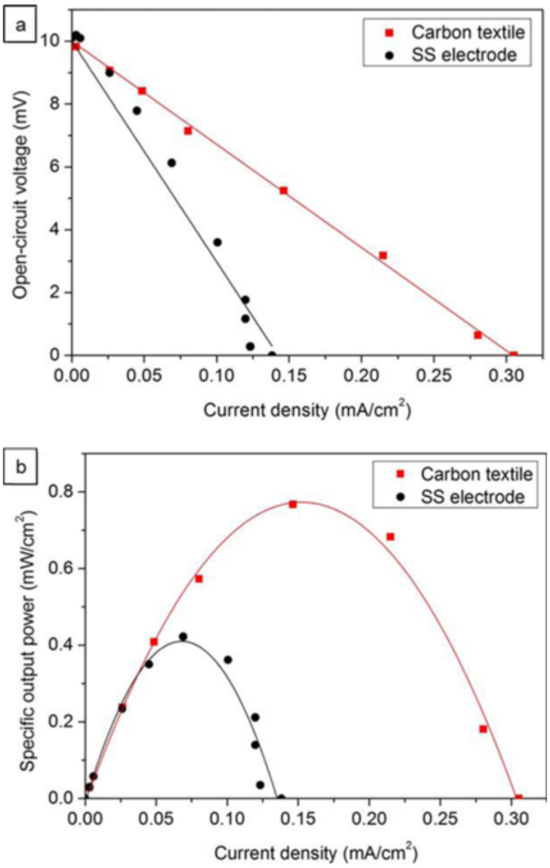

Fig. 4 (a) Comparison of discharge behaviors of the thermobattery using flat stainless steel and carbon textile electrodes. (b) Specific output power obtained from the E-I curve of Fig. 4(a)

Fig. 5(b) and (c) shows the E-I curves and the power generation from thermobatteries utilizing various electrodes of carbon textile (CT), carbon textile coated with SWNTs by 2 times (SWNT#2-CT) and 4 times (SWNT#4-CT). All experimental conditions and measurement setup were same as used in Fig. 4. The short-circuit current increased as the SWNT coating number increased (Fig. 5(b)), the maximum specific output power increased from 0.77 (CT) to 0.9 $\mu W/cm^2$ (SWNT#4-CT), as shown in Fig. 5(c). This improvement in power generation is obviously provided by SWNTs coated on the carbon textile. Moreover, a lower sheet resistance achieved by SWNT coating might reduce the ohmic overpotential of the thermobattery, which is mainly developed by the series resistances of electrode and electrolyte.[19] Therefore, for a given temperature difference and electrolyte concentration, the output current can be improved by the reduction of sheet resistance of electrodes.

The open-circuit potential in the thermobattery is basically determined by the temperature difference between the two electrodes. Electrical power generation depending on the temperature difference was evaluated by increasing the temperature at a hot electrode, while the temperature at a cold electrode was set to 5 °C. As the temperature difference increases from 5 to 8.5 °C with an increment of 2.14 °C, the open-circuit potential increased from 4 to 10 mV with the proportionality

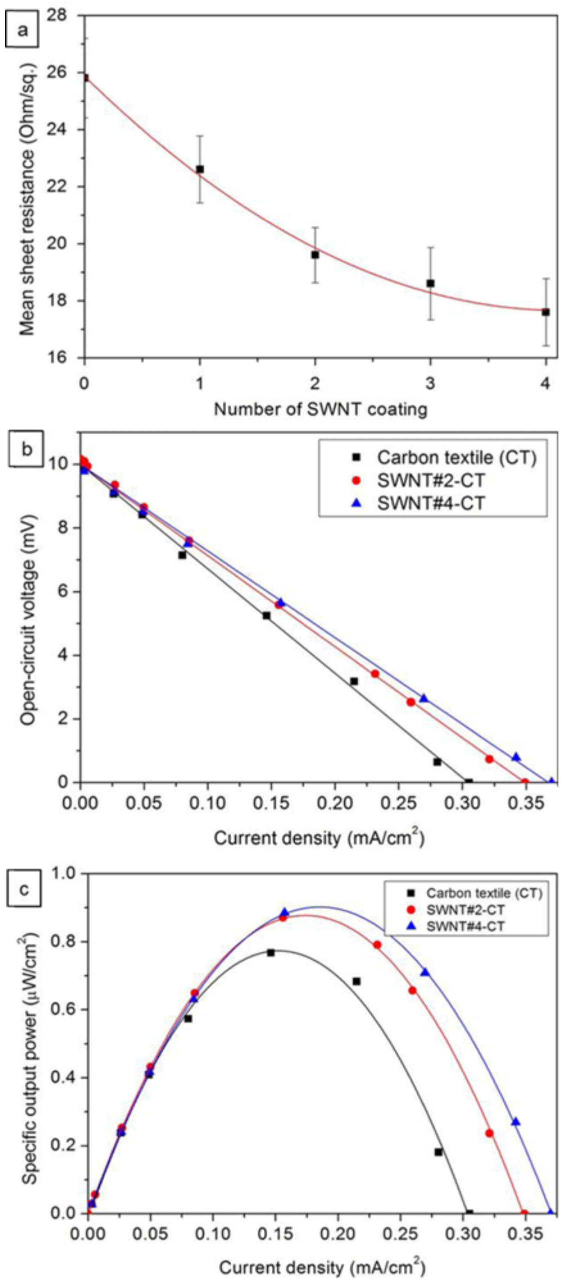

Fig. 5 (a) Variation of sheet resistance of carbon textile with respect to the SWNT coating number. (b) and (c) show the E-I curves and the specific output power from thermobatteries, respectively, utilizing various electrodes of carbon textile (CT), carbon textile coated with SWNTs by 2 times (SWNT#2-CT) and 4 times (SWNT#4-CT)

of thermoelectric coefficient of the electrolyte, resulting in an increase of the maximum power generation from 0.1 mW/cm^2 for ΔT=6.5°C to 0.88 mW/cm^2 for ΔT=8.5°C (Fig. 6). It is clear from the results of Fig. 6(b) that the maximum output power is quadratically proportional to the inter-electrode temperature difference.

4. Conclusion

We fabricated the coin-shaped thermobattery for scavenging waste thermal energy below a temperature of 100°C. The thermobattery utilizes temperature dependence of ferri/ferrocyanide redox potential and employs the SWNT coated carbon textile electrodes. Power generation of the thermobattery with carbon textile and flat stainless steel electrodes was compared to provide the effectiveness of carbon textile electrode. Owing to its high porosity and large specific surface area of carbon textile, the electrical output power was measured 2 times higher by employing carbon textile electrodes. To further improve the electrode performance, SWNT coatings on carbon textile were carried out. The sheet resistance of the carbon textile decreased remarkably as the SWNT coating number increased, showing ~1.5 reduction in sheet resistances from 25.8 to 17.6 ohm/sq. upon performing 4 times of SWNT coatings. The maximum specific output power in thermobattery increased from 0.77 (CT) to 0.9 μW/cm^2 (SWNT#4-CT). This improvement in power generation is attributed to an increase of the number of available reaction sites provided by SWNTs coated on the carbon textile. Moreover, a lower sheet resistance achieved by SWNT coating might reduce the ohmic overpotential of the thermobattery, which is mainly developed by the series resistances of electrode and electrolyte. Finally, the electrical power generation depending on temperature difference was evaluated, resulting in an increase of the maximum power generation from 0.1 mW/cm^2 for ΔT=6.5°C to 0.88 mW/cm^2 for ΔT=8.5°C.

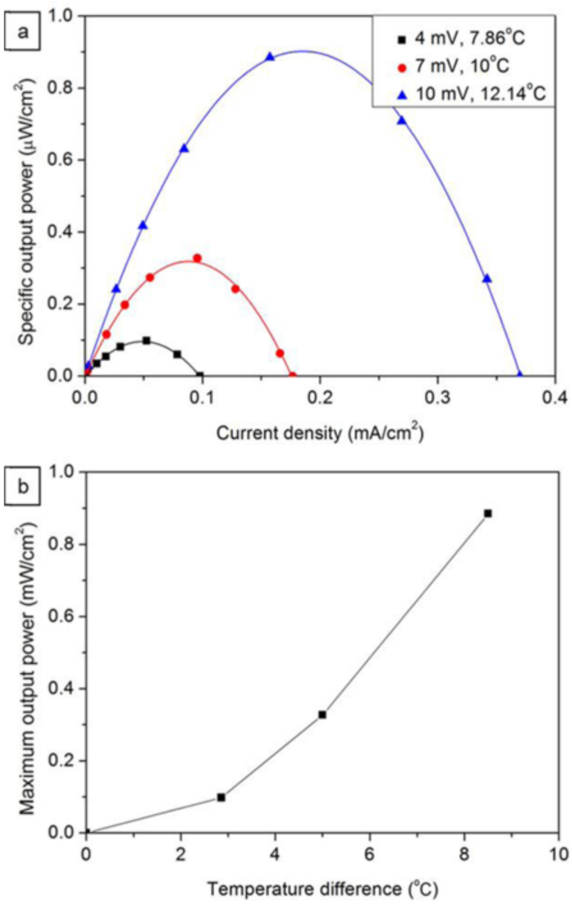

Fig. 6 (a) Evaluation of electrical power generation in thermobattery according to the inter-electrode temperature difference. (b) Maximum output power is plotted according to temperature difference

ACKNOWLEDGEMENT

This research was supported by the National Research Foundation of Korea (grants No. 2011-0024818), the Civil & Military Technology Cooperation Program through the National Research Foundation of Korea (NRF) funded by the Ministry of Science, ICT & Future Planning (No. 2013M3C1A9055407), "Development of Multi-Physics based Micro Manufacturing (MP-M2) technologies for Biomedical Projects" International Collaborative R&D Program project of Ministry of Knowledge Economy, "Development of Nano-level Surface Reformation Process and an Equipment using Ultrasonic Vibration" of the Ministry of Trade, Industry and Energy (MOTIE), and also supported by the 2012 Specialization Project Research Grant funded by the Pusan National University

REFERENCES

1. Hasnain, S. M., "Review on Sustainable Thermal Energy Storage Technologies, Part I: Heat Storage Materials and Techniques," Energy Conversion and Management, Vol. 39, No. 11, pp. 1127-1138, 1998.
2. Starner, T., "Human-powered Wearable Computing," IBM Systems Journal, Vol. 35, No. 3.4, pp. 618-629, 1996.
3. Paradiso, J. A. and Starner, T., "Energy Scavenging for Mobile And Wireless Electronics," IEEE Pervasive Computing, Vol. 4, No.1, pp. 18-27, 2005.
4. Bhandari, B., Poudel, S. R., Lee, K. T., and Ahn, S. H., "Mathematical Modeling of Hybrid Renewable Energy System: A Review on Small Hydro-Solar-Wind Power Generation," Int. J. Precis. Eng. Manuf.-Green Tech., Vol. 1, No. 2, pp. 157-173, 2014.
5. Bhandari, B., Lee, K. T., Lee G. Y., Cho, Y. M., and Ahn S. H., "Optimization of Hybrid Renewable Energy Power Systems: A Review," Int. J. Precis. Eng. Manuf.-Green Tech., Vol. 2, No. 1, pp. 99-112, 2015.
6. Bell, L. E., "Cooling, Heating, Generating Power, and Recovering Waste Heat with Thermoelectric Systems," Science, Vol. 321, No. 5895, pp. 1457-1461, 2008.
7. Gou, X., Xiao, H., and Yang, S., "Modeling, Experimental Study and Optimization on Low-temperature Waste Heat Thermoelectric Generator System," Applied Energy, Vol. 87, No. 10, pp. 3131-3136, 2010.
8. Hsu, C. T., Huang, G. Y., Chu, H. S., Yu, B., and Yao, D. J., "Experiments and Simulations on Low-temperature Waste Heat Harvesting System by Thermoelectric Power Generators," Applied Energy, Vol. 88, No. 4, pp. 1291-1297, 2011.
9. Navid, A., Vanderpool, D., Bah, A., and Pilon, L., "Towards Optimization of a Pyroelectric Energy Converter for Harvesting Waste Heat," International Journal of Heat and Mass Transfer, Vol. 53, No. 19-20, pp. 4060-4070, 2010.
10. Niu, X., Yu, J., and Wang, S., "Experimental Study on Low-Temperature Waste Heat Thermoelectric Generator," Journal of Power Sources, Vol. 188, No. 2, pp. 621-626, 2009.
11. Wu, C., "Analysis of Waste-Heat Thermoelectric Power Generators," Applied Thermal Engineering, Vol. 16, No. 1, pp. 63-69, 1996.
12. Yu, C. and Chau, K. T, "Thermoelectric Automotive Waste Heat Energy Recovery using Maximum Power Point Tracking," Energy Conversion and Management, Vol. 50, No. 6, pp. 1506-1512, 2009.
13. Ujihara, M., Carman, G. P, and Lee, D. G., "Thermal Energy Harvesting Device using Ferromagnetic Materials," Applied Physics Letters, Vol. 91, No. 9, Paper No. 093508, 2007.
14. Nam, S. K. and Lee, S. K., "The Effect of Ti Adhesion Layer on the Thermoelectric Noise of a High Resolution Thermopile for Nanowatt Heat Flux Sensor," Int. J. Precis. Eng. Manuf., Vol. 15, No. 11, pp. 2391-2396, 2014.
15. Kim, H., Lee, Y., and Lee, K. H., "Design of a Thermoelectric Layer for a Micro Power Generator," Int. J. Precis. Eng. Manuf., Vol. 13, No. 2, pp. 261-267, 2012.
16. Gunawan, A., Lin, C.-H., Buttry, D. A., Mujica, V., Taylor, R. A., et al., "Liquid Thermoelectrics: Review of Recent and Limited New Data of Thermogalvanic Cell Experiments," Nanoscale and Microscale Thermophysical Engineering, Vol. 17, No.4, pp. 304-323, 2013.
17. Hu, R., Cola, B. A., Haram, N., Barisci, J. N., Lee, S., et al., "Harvesting Waste Thermal Energy using a Carbon-nanotube-based Thermo-electrochemical Cell," Nano Letters, Vol. 10, No. 3, pp. 838-846, 2010.
18. Romano, M. S., Li, N., Antiohos, D., Razal, J. M., Nattestad, A., et al., "Carbon Nanotube-Reduced Graphene Oxide Composites for Thermal Energy Harvesting Applications," Advanced Materials, Vol. 25, No. 45, pp. 6602-6606, 2013.
19. Kang, T. J., Fang, S., Kozlov, M. E., Haines, C. S., Li, N., et al., "Electrical Power from Nanotube and Graphene Electrochemical Thermal Energy Harvesters," Advanced Functional Materials, Vol. 22, No. 3, pp. 477-489, 2012.
20. Bonetti, M., Nakamae, S., Roger, M., and Guenoun, P., "Huge Seebeck Coefficients in Nonaqueous Electrolytes," The Journal of Chemical Physics, Vol. 134, No.11, pp. 114513, 2011.
21. Kuzminskii, Y. V., Zasukha, V. A., and Kuzminskaya, G. Y., "Thermoelectric Effects in Electrochemical Systems. Nonconventional Thermogalvanic Cells," Journal of Power Sources, Vol. 52, No. 2, pp. 231-242, 1994.
22. Abraham, T. J., MacFarlane, D. R., and Pringle, J. M., "Seebeck Coefficients in Ionic Liquids-Prospects for Thermo-Electrochemical Cells," Chemical Communications, Vol. 47, No. 22, pp. 6260-6262, 2011.

23. Hu, L., Pasta, M., Mantia, F. L., Cui, L., Jeong, S., et al., “Stretchable, Porous, and Conductive Energy Textiles,” Nano Letters, Vol. 10, No. 2, pp. 708-714, 2010.

24. Kang, T. J., Choi, A., Kim, D. H., Jin, K., Seo, D. K., et al., “Electromechanical Properties of CNT-coated Cotton Yarn for Electronic Textile Applications,” Smart Materials and Structures. Vol. 20, No.1, Paper No. 015004, 2011.

25. Jiang, L., Gao, L., and Sun, J., “Production of Aqueous Colloidal Dispersions of Carbon Nanotubes,” Journal of Colloid and Interface Science, Vol. 260, No. 1, pp. 89-94, 2003.

26. Kang, T. J., Yoon, J. W., Kim, D. I., Kum, S. S., Huh, Y. H., et al., “Sandwich-Type Laminated Nanocomposites Developed by Selective Dip-Coating of Carbon Nanotubes,” Advanced Materials, Vol. 19, No. 3, pp. 427-432, 2007.

27. Hu, C. Y., Xu, Y. J., Duo, S. W., Zhang, R. F., and Li, M. S. “Non-Covalent Functionalization of Carbon Nanotubes with Surfactants and Polymers,” Journal of the Chinese Chemical Society, Vol. 56, No. 2, pp. 234-239, 2009.

28. Moore, V. C., Strano, M. S., Haroz, E. H., Hauge, R. H., and Smalley, R. E., “Individually Suspended Single-walled Carbon Nanotubes in Various Surfactants,” Nano Letters, Vol. 3, No. 10, pp. 1379-1382, 2003.

29. Luo, H., Shi, Z., Li, N., Gu, Z., and Zhuang, Q., “Investigation of the Electrochemical and Electrocatalytic Behavior of Single-wall Carbon Nanotube Film on a Glassy Carbon Electrode,” Analytical Chemistry, Vol. 73, No. 5, pp. 915-920, 2001.

30. Wang, J., Li, M., Shi, Z., Li, N., and Gu, Z., “Direct Electrochemistry of Cytochrome c at a Glassy Carbon Electrode Modified with Single-wall Carbon Nanotubes,” Analytical Chemistry, Vol. 74, No. 9, pp. 1993-1997, 2002.

31. Zhao, Q., Gan, Z., and Zhuang, Q., “Electrochemical Sensors based on Carbon Nanotubes,” Electroanalysis, Vol. 29, No. 9, pp. 1609-1613, 2010.